

## NUMERICAL ANALYSIS OF THE FLOW AND HEAT TRANSFER CHARACTERISTICS OF A STAGGERED PERFORATED LOUVER-FINNED HEAT EXCHANGER

by

**Kan CAO\***, Yaohua YUAN, Xiaomin LI,  
Chunyan WANG, and Zhiyong SU

School of Energy and Environment, Zhongyuan University of Technology, Zhengzhou, China

Original scientific paper  
<https://doi.org/10.2298/TSCI2303855C>

*A new kind of louvered fin structures with staggered holes is proposed, numerical simulation is carried out to study the heat transfer factor and the friction factor, and an experiment is designed to verify the simulation results at different Reynolds numbers, a good agreement is observed. Comparison with the traditional louver structure reveals that when the Reynolds number is between 150 and 400, the heat transfer factor increases by 10~24%, the friction factor increases by 1~2%, and the comprehensive evaluation factor increases by 9~23%. These results can be used for optimization of louver finned heat exchangers.*

**Key words:** louver fin, heat transfer performance, flow resistance performance, numerical simulation

### Introduction

Numerical methods are widely used to study complex problems, for examples, magnetic fluids [1], porous heat transfer [2], the single point incremental forming [3], double-layered oblique fins [4], Rabinowitsch fluids [5], and nanofluids [6]. Various iteration methods were used in the numerical simulation [7-9]. Fin-and-tube structures are widely used for heat exchangers [10], this paper focuses on the louvered fin heat exchanger, which is a parallel flow heat exchanger, and the louvered fins increase the airflow disturbance to strengthen the heat exchange [11]. This heat exchanger has a simple structure, small size, small weight, compact structure and other advantages, and it can greatly improve heat exchange efficiency in comparison with the traditional heat exchangers. Therefore, in recent years, many researchers performed much work on simulation and optimization [12, 13].

To enhance heat transfer, many methods have been adopted to improve the heat exchanger, for examples, slotting, surface punching, vortex generators or composite technology [14]. Dong *et al.* [15] conducted a relevant research on the heat transfer and flow resistance of louvered fins with different parameters on a wind tunnel test bench and found that fin length and fin spacing have a great impact on the heat transfer and resistance performance of fins, but fin height has a small impact. Zhou *et al.* [16] proposed an elliptical louvered-fin structure and proved numerically that the comprehensive performance factor can increase by 11~15% in comparison with the ordinary louvered structure under certain working conditions. Jiang [17] studied a heat exchange surface equipped with a slotted vortex generator through numer-

\* Corresponding author, e-mail: caokan96@163.com

ical simulation, from which it is found that a slotted vortex generator can not only effectively enhance heat transfer, but also effectively reduce thermal resistance. Kim *et al.* [18] presented a porous medium model for calculating the flow resistance on the side of louvered fins and effectively simulated the complex 3-D flow on louvered fins. Dogan *et al.* [19] performed an experimental comparison between double-row and three-row multiple louvered-fin heat exchangers, and the results showed that the heat exchanger with double-row fins has better validity and higher efficiency.

In this paper, a new type of louver finned heat exchangers is introduced, for which numerical simulation is made by CFD software and a comparison is made with the traditional louver finned heat exchanger, then the resistance and heat transfer characteristics of the staggered finned heat exchanger with perforated louvers are obtained, shedding a bright light on the future research on heat transfer enhancement of louvered heat exchanger.

### Model introduction

The heat exchanger with staggered perforated louvers has many advantages over the traditional louvered heat exchangers, the refrigerant passes through the flat tube and the manifold, and the air passes through the louver side. The refrigerant transfers heat to the flat tube, then to the louvered fins, and finally to the air.

The staggered perforated louver heat exchanger is characterized by symmetry and periodicity in structure, the simplified model is shown in figs. 1 and 2. Table 1 shows the parameters of traditional louvered fins.

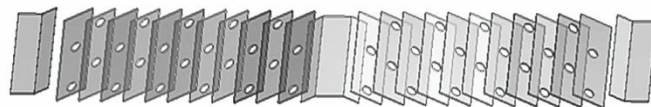


Figure 1. Schematic diagram of the staggered perforated louver fin

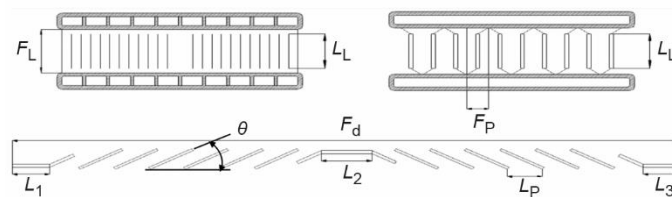


Figure 2. The structure of the staggered perforated louver-finned heat exchanger

Table 1. Basic parameters of the traditional louver fin

Item	Parameter value	Item	Parameter value
Fin spacing, $F_p$ [mm]	1.3	Louver angle, $\theta$ [°]	30
Louver length, $L_L$ [mm]	6.4	Inlet louver length, $L_1$ [mm]	1.4
Fin height, $F_L$ [mm]	7.4	Diversion zone length, $L_2$ [mm]	2.0
Fin width, $F_d$ [mm]	36.7	Outlet louver length, $L_3$ [mm]	1.4

### Governing equations

The governing equations are established as follows.

- Equation of continuity

$$\frac{\partial p}{\partial t}(\rho u_i) + \frac{\partial}{\partial x_i}(\rho u_i u_j) = S_m \quad (1)$$

- Equation of momentum conservation

$$\frac{\partial}{\partial t}(\rho u_i) + \frac{\partial}{\partial x_i}(\rho u_i u_j) = -\frac{\partial p}{\partial x_i} + \frac{\partial \tau_{ij}}{\partial x_j} + \rho g_i + F_i \quad (2)$$

- Equation of energy

$$\frac{\partial}{\partial t}(\rho E) + \frac{\partial}{\partial x_i}[u_i(\rho E + P)] = \frac{\partial}{\partial x_i} \left[ k_{\text{eff}} \frac{\partial T}{\partial x_i} - \sum_j h_j J_j + u_j (\tau_{ij})_{\text{eff}} \right] + S_h \quad (3)$$

where  $S_m$  is the source item,  $P$  - the static pressure,  $\tau_{ij}$  - the stress tensor,  $\rho g_i$  - the volume force of weight in  $i$ -direction,  $F_i$  - the volume forces of outside,  $k_{\text{eff}}$  - the effective heat transfer coefficient,  $J_j$  - the diffusion flow in  $j$ -direction, and  $S_h$  - the volume heat source.

### Boundary conditions

The boundary conditions are as follows: the inlet is the velocity boundary, and the air inlet temperature  $T_{\text{in}} = 293$  K, the outlet is the pressure outlet boundary, the upper and lower parts of the fluid domain are set as periodic boundaries, and the front and back of the pipe wall and fluid domain are constant temperature walls,  $T_w = 276.15$  K, and the contact surface between the fluid and fin is a coupling surface. The simple algorithm is used for the coupling of pressure and velocity, the second-order difference scheme is used for the momentum equation and energy equation, and the coupling calculation method is used for the heat conduction inside the fin and the fluid convection heat transfer between the fins [20].

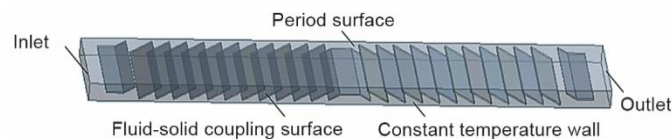


Figure 3. Boundary conditions of the traditional louvered fin

### Evaluation on comprehensive performance

The comprehensive performance factors are used to evaluate the performance of the heat exchanger.

The heat transfer factor  $j$  is expressed:

$$j = \frac{h_a}{\rho_a u_a C_{Pa}} \text{Pr}^{2/3} \quad (4)$$

where  $h_a$  [ $\text{Wm}^{-2}\text{K}^{-1}$ ] is the convective heat transfer coefficient of air,  $\rho_a$  [ $\text{kgm}^{-3}$ ] – the density of air,  $u_a$  [ $\text{ms}^{-1}$ ] – the velocity of air,  $C_{Pa}$  [ $\text{Jkg}^{-1}\text{K}^{-1}$ ] – the heat capacity of air, and  $\text{Pr} = 0.7$ .

The friction factor,  $f$ , is:

$$f = 2 \frac{\Delta P}{\rho_a \mu_a^2} \frac{d_e}{L} \quad (5)$$

where  $\Delta P$  [Pa] is the pressure decline,  $d_e$  [m] - the characteristic length which in this work is equal to fin pitch, and  $L$  [m] - the length of the channel.

The comprehensive factor  $E$  is:

$$E_{ij} = \frac{j}{f^{1/3}} \quad (6)$$

### Verification of numerical simulation

Numerical verification is of great importance in various fields, especially for those where the experiment is impossible, for examples, brain imagine [21-23]. To verify the accuracy of the simulation results, an experimental table of the heat pump air conditioning system of an electric bus is built, and the parallel flow heat exchanger is studied. The experiment table is built in the enthalpy difference laboratory of Zhongyuan University of Technology.



Figure 4. Parallel flow heat exchanger inside and outside the vehicle

In the experiment, the environmental changes inside and outside the vehicle are controlled by the console, and the operating parameters of the heat pump system are adjusted as shown in tab. 2 to meet the required operating conditions. Under the control of the computer, all data in the test process are collected at the same time.

Table 2. Geometric structure parameters of the traditional parallel flow heat exchanger

Item	Parameter value	Item	Parameter value
Outline dimension, [mm]	1900×586×36	Fin spacing, $F_p$ [mm]	1.3
Number of flat tubes	54	Number of pass	2
Size of flat tube, [m]	1850×36×3.25	Area, $A$ [m <sup>2</sup> ]	7.99
Louver length, $L_L$ , [mm]	6.4	Inlet fin length, $L_1$ [mm]	1.4
Fin width, $F_d$ , [mm]	36.7	Diversion zone length, $L_2$ , [mm]	2.0
Fin height, $F_L$ , [mm]	7.4	Louver angle, $\theta$ , [°]	30

Complete test data are obtained through testing and simulation, and the relationship among Reynolds number and the friction factor and heat transfer factor is shown in figs. 5 and 6.

Figure 5 shows that the maximum relative error of friction factor,  $f$ , are less than 11%, and the maximum relative error of heat transfer factor,  $j$ , is less than 17% in fig. 6, within the specified relative error value for engineering applications, *i.e.*,  $\pm 30\%$ . Therefore, the simulation results are acceptable.

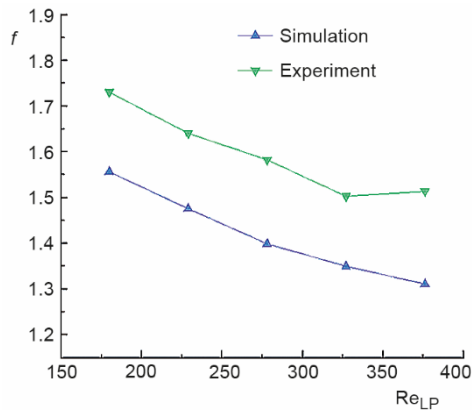


Figure 5. Friction factor  $f$ ; numerical and experimental results

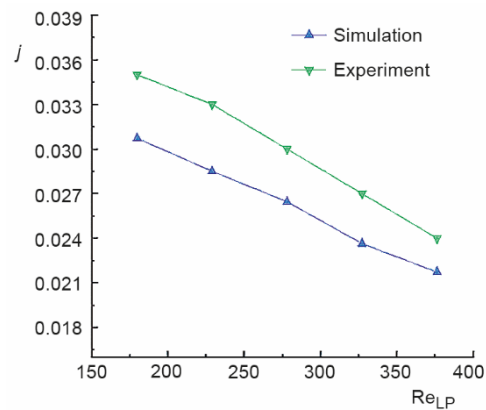


Figure 6. Heat transfer factor  $j$ ; numerical and experimental results

### Comparison of heat transfer performance between the two heat exchangers

Figure 7 shows the temperature contours of the traditional louver structure and the staggered perforated louver structure at  $Z = 0.024$  mm and  $Y = 0.001$  mm. The upper section of fig. 7 shows the contours of the traditional fin structure, its temperatures are 293 K and 286.91 K at the inlet and outlet, respectively, with a temperature drop of 6.09. The lower section shows the contours of the staggered perforated fin structure, its temperatures are 293 K and 285.29 K at the inlet and outlet, respectively, with a temperature drop of 7.71 K. The fin of the staggered perforated structure has a greater temperature drop than the traditional louver fin.

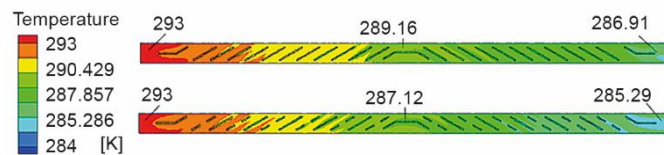


Figure 7. Comparison of temperature contours of the two fins at  $Z = 0.024$  mm

Figure 8 shows a comparison of the heat transfer factor between the traditional louver fin and staggered perforated louver fin. It can be found from the figure that under the research condition of  $Re = 150\sim 400$ , both decrease with the increase of Reynolds number, but the heat transfer factor of louvered fin of staggered perforated structure is higher than that of the ordinary louvered fin. Under operating conditions when Reynolds number is more than 300, the decreasing trend of the heat transfer factor of the perforated fin is significantly, but it is less than that of the ordinary fin. Therefore, the staggered perforated louver fin is better than the ordinary louver fin in terms of heat transfer.

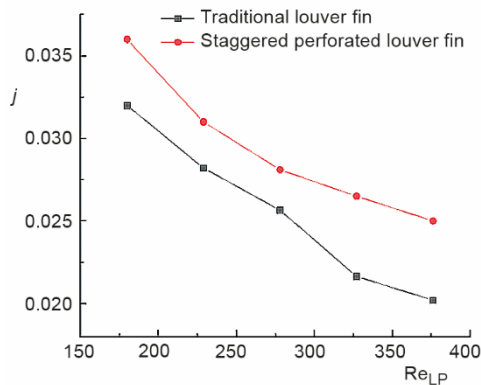


Figure 8. Comparison of heat transfer factor  $j$  of the two fins with Reynolds number

### Comparison of flow performance between the two heat exchangers

Figure 9 shows the pressure contours of the traditional louver structure and staggered perforated louver structure at  $Z = 0.024$  mm and  $Y = 0.001$  mm. The upper section of fig. 9 shows the contours of the traditional fin structure, its pressures are 60.86 Pa and 0.12 Pa at the inlet and outlet, respectively, with a pressure drop of 60.74 Pa. The lower section shows the contours of the staggered perforated fin structure, and the pressures are 61.11 Pa and 0.09 Pa at the inlet and outlet, respectively, with a pressure drop of 61.02 Pa. The fin of the staggered perforated structure has a slightly higher pressure drop than the traditional louver fin, but the gap is not very obvious.

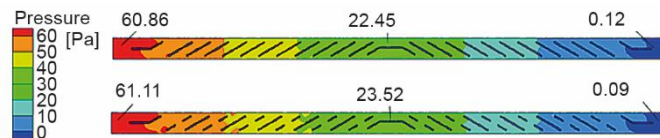


Figure 9. Comparison of pressure contours of the two fins at  $Z = 0.024$  mm

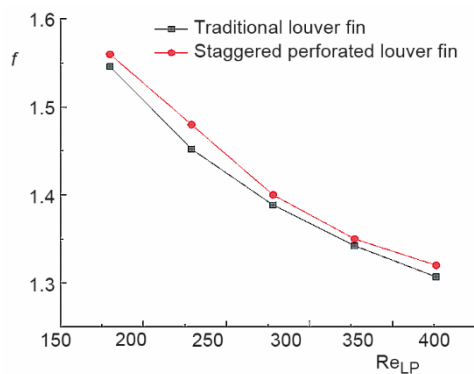


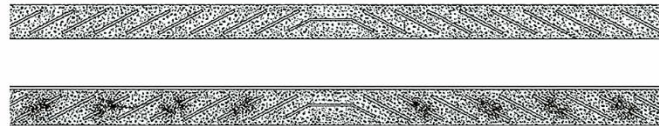
Figure 10. Comparison of friction factor of the two fins

Figure 10 shows the comparison of the friction factor of the traditional louver fin and staggered perforated louver structure. Under the research conditions of  $Re = 50\sim 400$ , both decrease with increasing Reynolds number, the friction factor of the louver fin of the staggered perforated structure is slightly higher than that of the ordinary louver fin, and the difference between the five detection points is only 1~2%. Under the operating conditions when Reynolds number is greater than 300, the friction factor of the perforated fin is gradually close to that of the traditional louver fin. Therefore, the staggered perforated louver fin has a slightly greater pressure drop than the ordinary louver fin.

### Comparison of comprehensive heat transfer performance between the two heat exchangers

Figure 11 shows the streamline tracking marking diagram of the two fins, which can well explain the reasons for the performance improvement of the new-type fin. It can be clearly found from the figure that compared with the traditional louver fin (above), the staggered

perforated louver fin (below) has a large amount of fluid flowing into the fin for heat transfer at the opening, which not only reduces the pressure drop but also enhances the heat transfer; and the mass of the heat exchanger is also reduced, so the performance of the fin is improved.



**Figure 11. Comparison of streamline tracking marks of the two fins at  $Z = 0.024$  mm**

According to the previous conclusions, compared with the traditional louver fin, the staggered perforated louver fin increase the heat transfer factor by 10~24% and a friction factor by 1~2%. Figure 12 shows the comparison of the comprehensive factors of the two fins when  $Re = 150\sim 400$ . It can be found from the figure that both comprehensive factors decrease with the increase of Reynolds number, but generally the staggered perforated louver fin has a greater comprehensive factor than that of the traditional louver fin by an increase 9~23% at the five detection points. When Reynolds number is greater than 270, the comprehensive factor of the traditional louver fin has a greater range of reduction, while the staggered perforated louver fin stabilizes gradually. Therefore, the staggered perforated louver fin has better performance than the traditional louver fin.

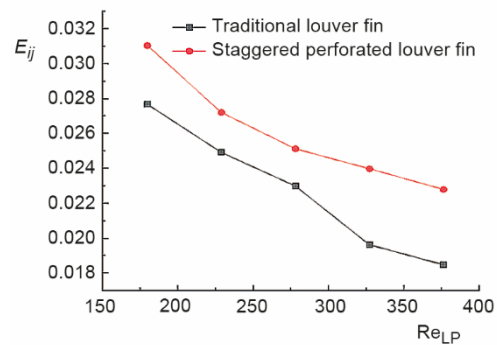


**Figure 12. Comparison of the two comprehensive factors  $E_{ij}$  with  $Re_{LP}$**

## Conclusion

This paper can obtain the following conclusions.

- Compared with the traditional louver structure, the staggered perforated louver structure has a small weight, it can save materials and meet the development needs of lightweight louvered-fin heat exchangers for vehicles.
- When the Reynolds number is 150~400, the staggered perforated louver fin has better heat transfer performance than the traditional louver fin, with a 10~24% increase.
- When the Reynolds number is 150~400, the comprehensive performance evaluation factor of the staggered perforated louver fin is better than that of the traditional louver fin, with a 9~23% increase.
- The above obtained results can be used for optimization [24-26] of louver finned heat exchangers in future.

## Acknowledgment

This work was supported by the National Natural Science Foundation Project (21776263).

## Reerence

- [1] He, J. H., et al., Non-linear Instability of Two Streaming-Superposed Magnetic Reiner-Rivlin Fluids by He-Laplace Method, *Journal of Electroanalytical Chemistry*, 895 (2021), Aug., 115388
- [2] He, C.-H., et al., A Fractal Model for the Internal Temperature Response of a Porous Concrete, *Applied and Computational Mathematics*, 21 (2022), 1, pp.71-77
- [3] Vosniakos, G.C., et al., Numerical Simulation of Single Point Incremental Forming for Asymmetric Parts, *Facta Universitatis-Series Mechanical Engineering*, 19 (2021), 4, pp. 719-734
- [4] Choong, J. Y., et al., Numerical Assessment on Heat Transfer Performance of Double-Layered Oblique Fins Micro-Channel Heat Sink with Al<sub>2</sub>O<sub>3</sub> Nanofluid, *Thermal Science*, 26 (2022), 1, pp. 477-488
- [5] He, J. H., Mostapha, D. R., Insight into the Significance of Hall Current and Joule Heating on the Dynamics of Darcy-Forchheimer Peristaltic Flow of Rabinowitsch Fluid, *Journal of Mathematics*, 2021 (2021), Oct., 3638807
- [6] He, J. H., et al., Insights into Partial Slips and Temperature Jumps of a Nanofluid Flow over a Stretched or Shrinking Surface, *Energies*, 14 (2021), 20, 6691
- [7] He, J. H., et al., Improved Block-Pulse Functions for Numerical Solution of Mixed Volterra-Fredholm Integral Equations, *Axioms*, 10 (2021), 3, 200
- [8] Nadeem, G. A., et al., New Optimal Fourth-Order Iterative Method Based on Linear Combination Technique, *Hacetatepe Journal of Mathematics and Statistics*, 50 (2021), 6, pp. 1692-1708
- [9] Wang, C. C., Yau, H. T., Application of a Hybrid Numerical Method to the Bifurcation Analysis of a Rigid Rotor Supported by a Spherical Gas Journal Bearing System, *Non-linear Dynamics*, 51 (2008), 4, pp. 515-528
- [10] Han, H., et al., A Numerical Study on Compact Enhanced Fin-And-Tube Heat Exchangers with Oval and Circular Tube Configurations, *International Journal of Heat and Mass Transfer*, 65 (2013), Oct., pp. 686-695
- [11] Wu, J. X., et al., Research on Enhanced Heat Transfer Performance of Air Side Louvered Fin of Air Cooler (in Chinese), *Refrigeration and Air-Conditioning*, 11 (2011), 4, pp.69-74
- [12] Kim, M. H., et al. Air-Side Thermal Hydraulic Performance of Multilouvered Fin Aluminum Heat Exchangers, *International Journal of Refrigeration*, 25 (2002), 3, pp. 390-400
- [13] Chang, Y. J., et al., A Generalized Friction Correlation for Louver Fin Geometry, *International Journal of Heat and Mass Transfer*, 43 (2000), 12, pp. 2237-2243
- [14] Zhu, M. S., et al., Research on the Application of Enhanced Heat Transfer Method in Heat Exchanger (in Chinese), *Energy and Energy Conservation*, 2 (2020), pp. 58-61
- [15] Dong, J. Q., et al., Experimental Study on Heat Transfer and Flow Resistance Characteristics of Louvered Fins (in Chinese), *Journal of Power Engineering*, 26 (2006), 6, pp. 871-874
- [16] Zhou, G. H., et al. Numerical Analysis of Heat Transfer Enhancement of Elliptical Louver Fins (in Chinese), *Cryogenics and Superconductivity*, 46 (2018), 6, pp. 71-75
- [17] Jiang, Y. C., et al., *Research on Flow and Heat Transfer Enhanced of in Tube with Concave Vortex Generator* (in Chinese), China University of Mining and Technology, Xuzhou, China, 2020
- [18] Kim, T. K., et al., A Porosity Model for Flow Resistance Calculation of Heat Exchanger with Louvered Fins, *Journal of Mechanical Science & Technology*, 30 (2016), 4, pp. 1943-1948
- [19] Dogan, B., et al., An Experimental Comparison of Two Multilouvered Fin Heat Exchangers with Different Numbers of Fin Rows, *Applied Thermal Engineering*, 91 (2015), Dec., pp. 270-278
- [20] Cao, W., et al., Numerical Simulation and Performance Analysis of Multi Structure Louver Fins: Numerical Simulation and Performance Analysis of Multi Structure Louver Fins (in Chinese), *Proceedings, 5<sup>th</sup> International Conference on Information Engineering for Mechanics and Materials*, Hohhot, Inner Mongolia Autonomous Region, China, 2015, pp. 573-578
- [21] Yu, W., et al., Tensorizing GAN with High-Order Pooling for Alzheimer's Disease Assessment, *IEEE Transactions on Neural Networks and Learning Systems*, 33 (2021), 9, pp. 4945-4959
- [22] You, S., et al., Fine Perceptive Gans for Brain MR Image Super-Resolution in Wavelet Domain, *IEEE Transactions on Neural Networks and Learning Systems*, On line first, <https://doi.org/10.1109/TNNLS.2022.3153088>, 2022
- [23] Hu, S., et al, Bidirectional Mapping Generative Adversarial Networks for Brain MR to PET Synthesis, *IEEE Transactions on Medical Imaging*, 41 (2021), 1, pp. 145-157
- [24] Perumal, S., et al., Heat Transfer Analysis in Counter Flow Shell and Tube Heat Exchanger Using Design of Experiments, *Thermal Science*, 26 (2022), 2A, pp. 843-848



- [25] Shen, Y. Y., *et al.*, Subcarrier-Pairing-Based Resource Optimization for OFDM Wireless Powered Relay Transmissions with Time Switching Scheme, *IEEE Transactions on Signal Processing*, 65 (2016), 5, pp. 1130-1145
- [26] Shen, Y., *et al.*, Convergence of Adaptive Nonconforming Finite Element Method for Stokes Optimal Control Problems, *Journal of Computational and Applied Mathematics*, 412 (2022), Oct., 114336